Basic Study on Similarity in Walking Machine from a Point of Energetic Efficiency

MAKOTO KANEKO, ASSOCIATE MEMBER, IEEE, SUSUMU TACHI, MEMBER, IEEE, KAZUO TANIE, MEMBER, IEEE, AND MINORU ABE

Abstract—**Because of the size of walking machines, scaled-down models having geometrical similarity can be used instead of full-scale models to measure energetic efficiency. First, to cope with this situation, five nondimensional parameters that control energetic efficiency of walking machines are introduced for nine physical parameters by applying dimensional analysis techniques. Next, in order to check those influences on energetic efficiency, computer simulations are performed for an *n*-legged walking model. In these simulations, the influence on ground reaction forces is considered to satisfy the approximate balance of forces and moments when an overall walking machine assembly is assumed as a free body. Resultantly, several new facts are acquired from the viewpoint of similarity law.**

I. Introduction

SPECIFIC resistance [1] is used as an index to evaluate the energy efficiency of walking machines. Specific resistance is a measurement of the amount of energy required to move a unit weight of a mobile body over a unit distance. The nondimensional parameter, having a clear concrete meaning, is used not only for artificial mobile machines but also in the field of zoological physiology. Since specific resistance means nondimensional consumed energy, the smaller the specific resistance number, the better the performance of mobile machines. Therefore, although specific resistance is somewhat remote from the concept of efficiency, this paper uses specific resistance as the index for evaluating the energy efficiency of walking machines.

The coordinate system showing specific resistance on the ordinate and average moving speed on the abscissa is known as the Gabrielle–von Karman diagram [2]. It is often used to compare the energy efficiency of artificial mobile machines [3], [4]. The purpose of plotting the specific resistance of walking machines on the Gabrielle–von Karman diagram is to provide intuitive, visual information to compare the specific resistance of walking machines with other kinds of artificial mobile machines. However, as the average moving speed used in the abscissa is a dimensional number, the similarity law cannot be applied.

On the other hand, because of the size of walking machines, scaled-down models having geometrical similarity can be used instead of full-scale models to measure specific resistance. In such a case, how can a direct relationship of specific resistance be obtained from a scaled-down model to a full-scale model? If this is impossible, what similarity law exists between the two? Although conventional walking machine research includes experimental specific resistance [5] considerations based on numerical simulation [6], studies based on similarity law have not been made. In the field of zoological physiology, although studies have been made of specific resistance using nondimensional parameters [7], they have potential defects, in that important nondimensional factors, such as body height, duty factor, and leg–body mass ratio, have not been taken into consideration.

To cope with these defects, six independent nondimensional parameters relating to a walking machine having two degrees-of-freedom with knee joints are introduced by applying dimensional analysis techniques. This paper further explains that certain combinations of these six nondimensional parameters can be converted into physically meaningful parameters such as specific resistance ϵ, leg–body mass ratio $\hat{m}$, stride ratio $\hat{s}$, nondimensional body height $\hat{h}$, nondimensional velocity $\hat{u}$, and duty factor β, which represents the ratio of support phase to one cycle. The leg systems are classified into two types according to the actuator arrangement, and numerical simulation is made for both leg systems to check the influences of each nondimensional parameter on the specific resistance. As a result, several new facts are acquired from the viewpoint of similarity law.

II. Introduction of Nondimensional Parameters

A. Assumptions for Dimensional Analysis

Now let us assume a walking model having knee joints as shown in Fig. 1. The following assumptions simplify the discussion, so as not to lose the true nature of the phenomena.

1) friction loss in joints shall be neglected;
2) actuator system is assumed not to have an energy storing system; and
3) mass distribution of the thigh and shank is assumed uniform.

B. Dimensional Analysis

For walking model shown in Fig. 1, a functional relationship is assumed as follows:

$$f(E, m_1, m_2, l, s, h, \bar{u}, g, T_0)=0. \tag{1}$$

Manuscript received June 21, 1985; revised May 12, 1986.

The authors are with the Robotics Department, the Mechanical Engineering Laboratory, Ministry of International Trade and Industry, Namiki 1-2 Tsukuba Science City, Ibaraki 305, Japan.

IEEE Log Number 8611968.

0882-4967/87/0200-0019$01.00

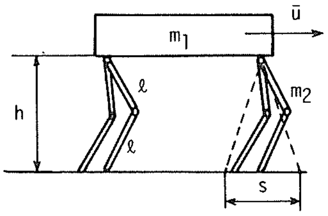

Fig. 1. Legged walking model (any number of legs is possible).

These physical values, except h, coincide with those used for the simulation study [6]. As for h, it is used as a parameter to determine the degree of insect type leg and mammal type leg and is considered a physical parameter having a great effect on consumed energy E. Therefore in this paper, dimensional analysis is conducted with h included. Besides these physical parameters, several parameters relating to the geometry of the body of walking machines influence the consumed energy, but in this paper, this influence is considered a secondary effect compared with the above physical parameters, and therefore neglected. Although m_1 and m_2, or l, s, and h in (1) have the same dimension, their influence on the physical phenomena are considered differently. Therefore each parameter cannot be used independently as a representative parameter. This idea is based on the concept of directional dimensional analysis. According to Buchingham's π theorem [8], (1) and (2) are equivalent.

$$\psi(\pi_1, \pi_2, \pi_3, \cdots \pi_p)=0 \quad (2)$$

As the physical value that controls the function f is represented by a combination of the units of mass $[M]$, length $[L]$, and time $[T]$, π_i is a nondimensional parameter consisting of a combination of less than four physical parameters. As there are nonzero determinants among the cubic determinants obtained from the dimensional matrix which has $[M]$, $[L]$, and $[T]$ on the row and the physical parameters selected from (1) on the column, the rank of the dimensional matrix becomes three. Therefore p becomes six, which is obtained by deducting the number of units from the number of physical parameters. This indicates that six independent nondimensional parameters exist.

Assuming the relationship

$$E^{K1} m_1^{K2} m_2^{K3} l^{K4} s^{K5} h^{K6} \bar{u}^{K7} g^{K8} T_0^{K9} = \text{nondimensional} \quad (3)$$

can be established, dimensional analysis provides the following six nondimensional parameters:

$$\pi_1 = \frac{E}{m_1 g l} \qquad \pi_2 = \frac{m_2}{m_1}$$

$$\pi_3 = \frac{s}{l} \qquad \pi_4 = \frac{h}{l}$$

$$\pi_5 = \frac{\bar{u}}{\sqrt{gl}} \qquad \pi_6 = T_0 \sqrt{\frac{g}{l}}$$

B. Modified Nondimensional Parameters and Their Physical Meanings

The physical meanings of the six nondimensional parameters obtained in the preceding section are unclear as they are.

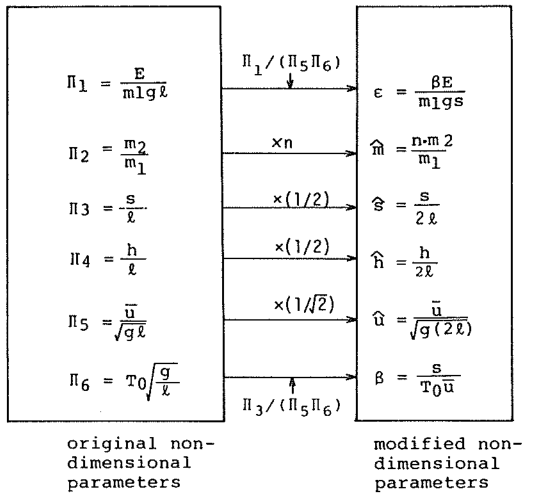

Fig. 2. Modified nondimensional parameters.

In general, six independent nondimensional parameters obtained from dimensional analysis are not the only possible form. For example, body height h can be used instead of leg unit length l in π_3. It is equivalent to the idea that assumed π_3/π_4 is an independent nondimensional parameter instead of π_3. Such a permutation is permitted because the concept is based on the idea that the independence of the six nondimensional parameters can be maintained even though they are multiplied by or divided by factors. In this section the nondimensional parameters obtained are modified into physically meaningful forms by multiplying them by appropriate factors or combining them. Then the physical meanings of those parameters obtained is discussed. Modified nondimensional parameters in Fig. 2 are based on this philosophy (n represents the number of legs). When specific resistance is indicated by ϵ, it is represented by a formula $\epsilon = E/(m_1 g B)$ [6]. Whereas B ($= s/\beta$) is the movement of the center of gravity of the body during one cycle, $\pi_1/(\pi_5 \cdot \pi_6)$ is a nondimensional parameter, which coincides with the definition of ϵ. π_2 is a nondimensional mass ratio (the mass of one leg/the mass of the body), but generally $\hat{m}$, which is obtained by dividing the mass of legs by the mass of body instead of π_2, is more convenient. If $\hat{m}$ is used, the approximate influence due to the number of legs can be deleted in an evaluation of the energy consumed by the leg system. On the other hand, the leg unit length l is used for the typical length of a walking machine in π_3, π_4, and π_5. The leg length, or $2l$, is used for the typical length in the corresponding nondimensional parameters; i.e., stride ratio $\hat{s}$, nondimensional height $\hat{h}$, and nondimensional velocity $\hat{u}$. The leg length $2l$ presents a more perceptive image of the typical length of a walking machine than the leg unit length l. The nondimensional velocity $\hat{u}$ essentially coincides with the Froude number [8]. Its physical meaning is that it indicates the ratio of the inertial force to gravitational force. When the Froude number is considered in relationship to a walking machine, it means the ratio of the centrifugal force $m_1\bar{u}^2/(2l)$ generated at the hip by the rotating motion of the body about the toe in the support phase against the gravitational force $m_1 g$ (it is assumed that the body makes a rotating motion of radius $2l$ having the center at the foot tip). Therefore, as the Froude number (or nondimensional velocity $\hat{u}$) approaches 1, a walking motion, in which at least one leg remains on the ground in the support phase, cannot be maintained, and the gait changes from walking to running. The change of the gait according to the changing Froude number has been pointed out by R. M. Alexander [7]. For walking machines premised on static stability, $\hat{u}$ is assumed to be sufficiently smaller than 1. Finally, by making $\pi_3/(\pi_5, \pi_6)$ a new nondimensional parameter instead of π_6, the duty factor β (the ratio of time when the legs are in the support phase to one cycle) can be derived, which is an important parameter controlling the motion of a walking machine. The duty factor influences the specific resistance from the aspects of the kinetic energy of the transfer leg and the movement of the center of gravity of the body during one cycle.

Therefore, the specific resistance can be indicated by (4) as a function of five modified nondimensional parameters:

$$\epsilon = \epsilon(\hat{m}, \hat{s}, \hat{h}, \hat{u}, \beta). \tag{4}$$

III. Computer Simulation

To investigate the influence each nondimensional parameter has on the specific resistance, this section discusses computer simulation using an n-legged walking model having two degrees-of-freedom for each leg.

As for research of simulation of specific resistance, conventional research was performed using a very simple model by S. Hirose *et al.* [6]. However, since scale effects are not considered in [6], the simulation results are only available for a limited scale machine. The simulation in this paper especially takes the following conditions into consideration.

1) Based on the similarity law, all the results are indicated in nondimensional parameters.
2) The influence of the difference in the arrangement of actuators on specific resistance is discussed.
3) The effect of the inertia reaction force of the ground is discussed in order to satisfy the approximate balance of forces and moments when an overall walking machine assembly is assumed as a free body.
4) The effect of nondimensional height $\hat{h}$ is examined.

A. Considerations on Arrangement of Actuators

The arrangement of actuators of walking machines are classified into two types as shown in Fig. 3. One type shown in Fig. 3(a) is such that the rotation of the thigh actuator drive shaft makes the fixed side of the shank actuator rotate at the same angle. This type is called a relative coordinate system (RCS) arrangement in this paper. Another type shown in Fig. 3(b) is such that regardless of the rotation of the thigh actuator drive shaft, the fixed side of shank actuator points in the same direction. This type is called body coordinate system (BCS) arrangement in this paper. The muscle–bone system of living things including animals and the legs of various walking machines have RCS actuator arrangement. As indicated in Fig. 3(b), BCS actuator arrangement is limited to artificial legs. Although the specific resistance of BCS actuator arrangement has been examined [6], the specific resistance of RCS actuator arrangement has not been examined except the massless model ($m_2 = 0$) [7]. For example, let us assume a case in which supporting force F acts as the reaction force of the ground, with the mass of the legs assumed zero, as shown in Fig. 3. In the case of RCS arrangement, magnitude of the moment acting on the hip joint is expressed by the product of the supporting force F and Δx (Δx is the horizontal distance between the supporting point and the hip joint). In the case of BCS arrangement, the magnitude of the moment acting on the hip joint appears as if a vertical force F acted on the knee joint. Therefore the difference in the actuator arrangements should impose a decisive influence on the specific resistance.

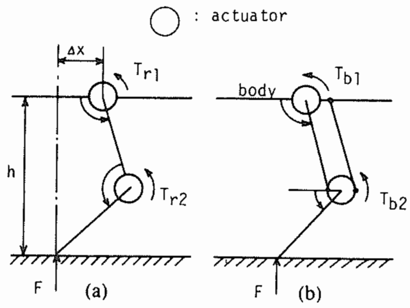

Fig. 3. Two types of actuator arrangement. (a) Relative coordinate system (RCS): The muscle-bone system of living things including animals has this type of actuator arrangement. (b) Body coordinate system (BCS): BCS actuator arrangement is limited to artificial legs.

B. Assumption for Analysis

Now we will discuss an n-legged walking model (Fig. 4) and its coordinate system. To simplify the analysis, the following assumptions are made.

Assumption 1: The actuator characteristics are given by (5) according to [6]. Thus

$$P = \delta\langle P'\rangle = \begin{cases} P' & P' > 0 \\ 0 & P' \leqq 0 \end{cases} \tag{5}$$

where P' is the drive power to be generated at each joint and P represents the power consumption of the actuator of each joint.

Assumption 2: The body makes a constant speed and horizontal motion.

Assumption 3: The foot in the transfer phase returns close onto the ground.

Assumption 4: An even number of legs is provided.

Assumption 5: The legs make a reciprocating motion close to the body.

Assumption 6: The body is sufficiently long as compared with the body height.

Assumption 7: Ground reaction forces with the same magnitude act on the legs on the same side of the body in the support phase.

Generally, walking machines have one more freedom related to overall leg rotation around x-axis in each hip. However, this freedom is not absolutely necessary for generating normal walking pattern, but necessary for avoiding obstacles and body rotating. Therefore, the legged walking model with two degrees-of-freedom legs as shown in Fig. 4 can keep the

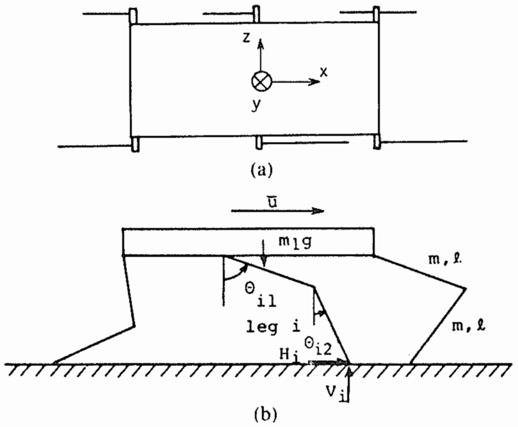

Fig. 4. A legged walking model and its coordinate system. (a) Top view. (b) Side view.

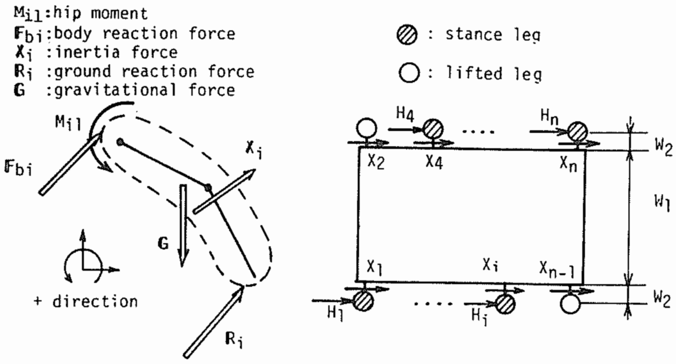

Fig. 5. Free body diagram of the model. (a) Free body diagram for ith leg. (b) Horizontal-force balance.

generalization for analysis of the energetic efficiency in normal walking.

Assumption 1 is equivalent to the phenomena that the actuator consumes power in the positive work mode and does not consume power in the isometric negative work mode [6].

Assumptions 2 and 3 suppose that simulation tests are performed with the energy consumption of the actuator at zero or a minimum, which relates to changes in the potential energy of the body and the leg system. Both assumptions are established to simplify analysis. On the other hand, if the number of the legs in the support phase is more than four, determination of the ground reaction force becomes an indeterminable problem, and the force generally cannot be determined uniformly. As for the horizontal reaction force, the calculation becomes indeterminable even if the number of the legs in the support phase is three. Assumptions 5–7 are established to satisfy the equations of balancing of the forces of the overall body, and of the moments approximately. Details are explained in Section D.

C. Introduction of Joint Moment

The equation of motion about leg i of a walking model in Fig. 5 is expressed by (6), and the ground reaction force vector is represented by $\boldsymbol{R}_i$;

$$A_i\ddot{\boldsymbol{\theta}}_i + B_i\dot{\boldsymbol{\theta}}_i^2 + C_i \sin \boldsymbol{\theta}_i + D_i\boldsymbol{R}_i = \boldsymbol{M}_i \tag{6}$$

where

$$\ddot{\boldsymbol{\theta}}_i = [\ddot{\theta}_{i1}, \ddot{\theta}_{i2}]'$$

$$\dot{\boldsymbol{\theta}}_i^2 = [\dot{\theta}_{i1}^2, \dot{\theta}_{i2}^2]'$$

$$\sin \boldsymbol{\theta}_i = [\sin \theta_{i1}, \sin \theta_{i2}]'$$

$$\boldsymbol{R}_i = \begin{cases} [H_i, V_i]', & \text{(support phase)} \\ [0, 0]', & \text{(transfer phase)} \end{cases}$$

$$\boldsymbol{M}_i = [M_{i1}, M_{i2}]'$$

The coefficient matrices A_i, B_i, C_i, and D_i are dependent on the actuator arrangement and are given in Appendix A. In (6), when a foot motion trajectory that will realize a constant-speed horizontal motion is assumed, angles $\boldsymbol{\theta}_i$ of each joint, angular velocity $\dot{\boldsymbol{\theta}}_i$, and angular acceleration $\ddot{\boldsymbol{\theta}}_i$ are determined uniformly. As each coefficient matrix becomes the function of θ_{ij} (i = 1 to n, j = 1, 2), all the factors except the ground reaction force vector $\boldsymbol{R}_i$ become known values.

D. Introduction of the Ground Reaction Force

With the ith leg body reaction force and the inertia force represented by $\boldsymbol{F}_{bi} = [X_{bi}, Y_{bi}]'$ and $\boldsymbol{X}_i = [X_i, Y_i]'$ respectively as shown in Fig. 5(a), the gravity force $\boldsymbol{G}_i = [0, -2mg]'$, (7) can be established.

$$\boldsymbol{F}_{bi} + \boldsymbol{X}_i + \boldsymbol{G}_i + \boldsymbol{R}_i = 0. \tag{7}$$

Then, by adding (7) for leg 1 through leg n and dividing the sum into x and y components, (8) and (9) are obtained. The positive direction of the force, and the moment is shown in Fig. 5. Thus

$$\Sigma(X_{bi} + X_i + H_i) = 0 \tag{8}$$

$$\Sigma(Y_{bi} + Y_i + V_i - 2mg) = 0. \tag{9}$$

According to assumption 2, as the body makes a constant speed horizontal motion

$$\Sigma X_{bi} = 0,\ \Sigma Y_{bi} = -m_1 g. \tag{10}$$

Therefore, (8) and (9) are converted into (11) and (12).

$$\Sigma(X_i + H_i) = 0 \tag{11}$$

$$\Sigma(Y_i + V_i) = (m_1 + 2mn)g. \tag{12}$$

Because X_i and Y_i are inertia forces, they become known values when the motion of the foot is determined. Equations of balance of the moments about each axis having the center of gravity of the body as the origin are expressed as the following (13)–(15).

$$\Sigma(H_i + X_i)z_i = 0 \tag{13}$$

$$\Sigma(V_i + Y_i)z_i = 0 \tag{14}$$

$$\Sigma[H_i h + X_i h_i + (V_i + Y_i)x_i] = 0. \tag{15}$$

However, (15) can be established for primary approximation.

And h_i is y coordinate of the acting point of the inertia force. Regarding (11)–(15), for very slow walking, $H_i = 0$, $\Sigma V_i = (m_1 + 2mn)g$, $\Sigma V_i z_i = 0$, and $\Sigma V_i x_i = 0$, which coincide with the equations that C. A. Klein *et al.* [9] are using for the force control of six-legged walking machines. Now, for a three-leg supporting system, which corresponds to the minimum number of legs required to maintain static stability, each reaction force becomes an indeterminable problem and cannot be determined uniformly because (11)–(15) provide only five equations for six unknown values. One of the methods to solve such an indeterminable problem is the pseudo-inverse method, which is based on a philosophy that the norm of solution is made minimum. However, as z_i provides $z_{2i} = W_1/2$, $z_{2i-1} = -W_1/2$ due to its symmetry, (13) and (14) do not practically rely on the size of W_1. However, since (15) contains coordinate value x_i in the direction of x, concrete numerical values must be given for the geometrical shape of the body of a walking body to use this method. Therefore, by applying the pseudo-inverse method to (11) and (13), (16) gives the horizontal reaction force with H representing the horizontal reaction force vector. Thus

$$H = A'(AA')^{-1}\boldsymbol{b}. \tag{16}$$

However, A as a coefficient matrix consists of (11) and (13), and $\boldsymbol{b} = (-\Sigma X_i, -\Sigma X_{2i} + \Sigma X_{2i-1})'$. Actual calculation of (16) using (11) and (13) indicates that horizontal reaction forces of the same magnitude act on the legs on the same side in the support phase. Applying the pseudo-inverse method to (12) and (14) achieves the same result. Among the elements of (15), V_i generally has the largest value, which correlates with the body mass, but if the body is long enough (assumption 6), and the legs in the support phase are distributed evenly fore and aft of the body, it is generally supposed that similar size vertical reaction forces act on the legs on one side in the support phase. That is to say, it is predicted that there will be no remarkable difference between the two solutions even if pseudo-inverse solutions obtained with (15) are taken into consideration. Therefore this paper sets assumption 7 from the viewpoint of the simplification of the problem.

Based on the above philosophy, (17) expresses the horizontal reaction force:

$$\begin{cases} H_{2i} = -\sum_{i=1}^{n/2} X_{2i}/n_1 \\ H_{2i-1} = -\sum_{i=1}^{n/2} X_{2i-1}/n_2. \end{cases} \tag{17}$$

where n_1 and n_2 are the number of the legs in the support phase at even number leg row and odd number leg row, respectively. A similar idea gives (18) for the vertical reaction force:

$$\begin{cases} V_{2i} = \left[(m_1 + 2mn)g/2 - \sum_{i=1}^{n/2} Y_{2i}\right] / n_1 \\ V_{2i-1} = \left[(m_1 + 2mn)g/2 - \sum_{i=1}^{n/2} Y_{2i-1}\right] / n_2 \end{cases} \tag{18}$$

E. Introduction of Specific Resistance

This section introduces the equation of specific resistance using the joint moment M_i, which is obtained by the procedures up to Section III-D, to calculate the consumed power of the actuators.

First, let us assume an RCS actuator arrangement. Assuming that angular velocity of the actuator of joint j of leg i as $\dot{\alpha}_{ij}$, $\dot{\alpha}_i = [\dot{\alpha}_{i1}, \dot{\alpha}_{i2}]'$ can be expressed as (19) using $\boldsymbol{\theta}_i = [\theta_{i1}, \theta_{i2}]'$ of Fig. 4:

$$\dot{\alpha}_i = K\dot{\boldsymbol{\theta}}_i. \tag{19}$$

K is given in Appendix B.

Therefore, the power consumed by the actuator of joint j of leg i and the energy E to be consumed by all the legs during one cycle are indicated by (20) and (21), respectively:

$$P_{ij} = \delta\langle M_{ij} \cdot \dot{\alpha}_{ij}\rangle \tag{20}$$

$$E = \int_0^{T_0} \sum_{i=1}^{n} \sum_{j=1}^{2} P_{ij}\, dt. \tag{21}$$

Therefore, based on the definition [6], (22) represents the specific resistance:

$$\epsilon = \frac{\beta E}{m_1 g s}. \tag{22}$$

Further, specific resistance corresponding to BCS arrangement can be obtained by using BCS joint moment M'_{ij} and K' (Appendix B) in place of K.

F. Numerical Calculation

The calculation procedure described up to Section III-E is summarized by the flow chart shown in Fig. 6. The flow chart shows numerical calculations for three kinds of foot time charts shown in Fig. 7. Fig. 7 shows the relative foot velocity against the body. Fig. 7(a) shows a case where changes of the foot velocity becomes discontinuous when $t = (1 - \beta)T_0$. This cannot be used unless the leg mass is zero ($\hat{m} = 0$). If $\hat{m} \fallingdotseq 0$, a joint moment of an infinite value generates when $t = (1 - \beta)T_0$. Fig. 7(b) shows the most simple time chart without physical contradiction even when $\hat{m} \fallingdotseq 0$. In this case, although the joint moment becomes discontinuous, it does not become infinite. Furthermore, Fig. 7(c) shows a concept that makes even the joint moment continuous. In this paper, time charts of Fig. 7(b) and (c) are called type 1 and type 2, used for the calculations in a case of $\hat{m} \fallingdotseq 0$. Equation (23) gives the time chart for type 2:

$$\begin{aligned} &\text{(i)}\ 0 \leqq t \leqq (1-\beta)T_0 \\ &u = \frac{15}{8}\bar{u}\left\{\frac{1}{1-\beta}\left(\frac{t}{T_1}-1\right)^4 - \frac{2}{1-\beta}\left(\frac{t}{T_1}-1\right)^2 + \frac{1}{1-\beta} - \frac{8}{15}\right\} \\ &\text{(ii)}\ (1-\beta)T_0 \leqq t \leqq T_0 \\ &u = -\bar{u} \end{aligned} \tag{23}$$

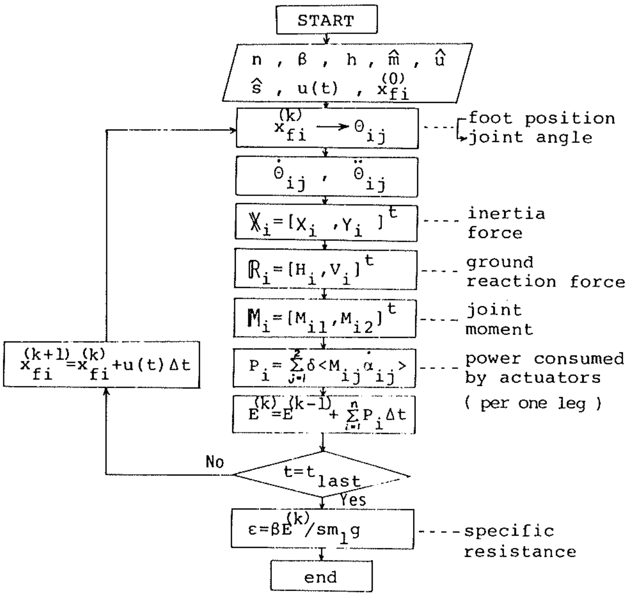

Fig. 6. Flow chart for simulation.

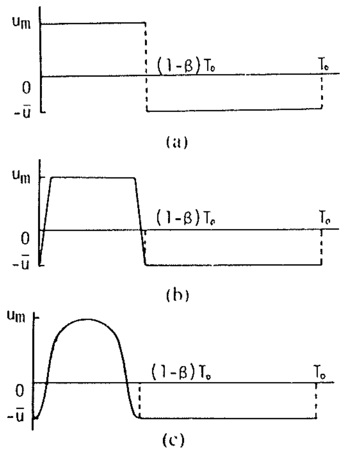

Fig. 7. Foot relative velocity time chart for simulation.

where $T_1 = (1 - \beta)T_0/2$.

The next step is to define the stride s of a walking model. Stride s for $\hat{h} < 0.5$ is defined as shown in Fig. 8(a). Therefore the mobility range of the foot is expressed by $[\sqrt{\hat{h} - \hat{h}^2}, \sqrt{\hat{h} - \hat{h}^2} + \hat{s}]$ using a nondimensional coordinate system having its origin at the hip joint, and thereby $\hat{s}_{\max} = \sqrt{1 - \hat{h}^2} - \sqrt{\hat{h} - \hat{h}^2}$ is introduced. The definition is so made that, when $\hat{h} > 0.5$, the foot makes a reciprocating motion having its center at the hip joint as shown in Fig. 8(b). Therefore the mobility range of the foot becomes $[-\hat{s}/2, \hat{s}/2]$, and $\hat{s}_{\max} = 2\sqrt{1 - \hat{h}^2}$.

The results of calculations when the leg mass is zero ($\hat{m} = 0$), which are carried out to check the program, are shown in Fig. 9(a) and (b), which are of the RCS-type actuator arrangement. Fig. 9(c) shows a BCS-type actuator arrangement. In Fig. 9, the solid line indicates the analytical solution. Numerical integration including the above solution is generally called analytical solution. The alternate long and short dotted line indicates the linear analytical solution based on an assumption that the stride is small compared to the leg length.

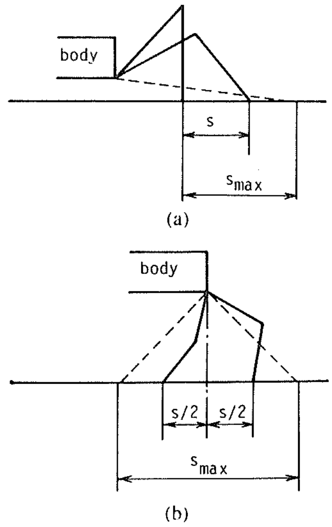

Fig. 8. Definition of leg stride length and mobility range of foot. (a) $\hat{h} < 0.5$. (b) $\hat{h} > 0.5$.

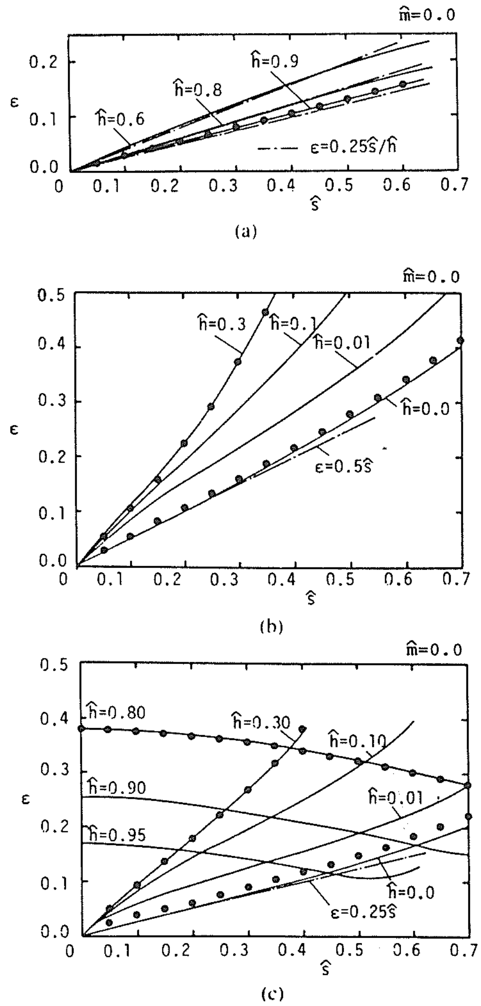

Fig. 9. Specific resistance in $\hat{m} = 0$. The solid line indicates the analytical solution. The alternate long and short dotted line indicates the linear analytical solution based on an assumption that the stride is small compared to the leg length. The solid dots indicate the numerical solution based on Fig. 6. (a) RCS. (b) RCS. (c) BCS.

These calculations are given in Appendix C. The solid dots represent the numerical solution obtained from calculation based on Fig. 6. In this case the calculation was made based on an assumption that, in order to make correspondence with the analytical solution, the ground reaction force is distributed evenly to all the legs in the support phase. Comparison of these results clearly indicates that all results fairly agree.

Let us examine the calculation results for $\hat{m} = 0$. In the case $\hat{h} < 0.5$, the specific resistance is in approximate proportion to the stride ratio $\hat{s}$. The specific resistance of RCS type arrangement becomes greater than that of BCS type arrangement, and approximately doubles when $\hat{h} \to 0$. In case $\hat{m} = 0$, the work of the hip joint and the knee joint have equal magnitude with opposite signs. The reason that the specific resistance of RCS type doubles that of BCS type when $\hat{h} \to 0$, corresponds to the fact that the knee joint angular change for the same knee joint moment differ in double magnitude. When $\hat{h} > 0.5$, the specific resistance of either RCS or BCS type becomes smaller as $\hat{h}$ approaches 1. Contrary to that, ϵ is in approximate proportion to $\hat{s}$ for the RCS type, and the following approximate relationship can be established for BCS type; i.e., $\epsilon = a - b\hat{s}\,(a > 0,\, b > 0)$. Physical interpretation of this result is described in Appendix D in detail. The model of BCS type for which $\hat{h} \to 0$ is assumed corresponds to the insect type mentioned in [6], and, of course, the results of both types agree. The consumed energy does not become zero, although based on an assumption of constant horizontal motion speed of the body with the mass of the legs at zero because of the actuator model. As a detailed explanation of this phenomenon is presented by [6], to exclude nuisance duplication, this paper does not discuss this problem.

Then, let us examine a case where $\hat{m} \fallingdotseq 0$. As the influence of nondimensional height $\hat{h}$ on the specific resistance for $\hat{m} = 0$ is almost known, nondimensional height $\hat{h}$ for the following calculations will be given typical fixed values of $\hat{h} = 0.002$ and $\hat{h} = 0.9$ for insect type and mammal type, respectively.

Fig. 10 shows the effects of the inertia reaction force on the specific resistance investigated using the time chart for type 1. The solid line indicates data for which the inertia reaction force is taken into account, and the dotted line shows when the force is neglected. Fig. 10 indicates that the effects of the inertia reaction force on the specific resistance is unexpectedly large. The information given by Fig. 10 can be interpreted as a nondimensional form of Gabrielle–von Karman Diagram.

Fig. 11 shows the results of calculation made in concurrence with the data of [6] in an attempt to compare with the existing calculation results. The solid line indicates data for which the effects of the inertia reaction force are taken into account, and the dotted line indicates when the force is neglected. The numerical calculation was made for the time charts of types 1 and 2. The calculation result using type 2 time chart gives generally large values because the maximum speed is about three times that of type 1 to obtain a smooth-speed change. The calculation results of types 1 and 2, which exclude the inertia reaction force (dotted lines) aptly put between the calculation results of [6] (with inertia reaction force neglected), suggest adequacy of the calculation results.

Fig. 12 shows the results of examination of the duty factor effects using the time chart of type 1. Fig. 12 indicates that the duty factor affects the specific resistance seriously. Now, $\beta = 0.75$ and $\beta = 0.5$ are the minimum values permitting static stability of four-legged and six-legged walking machines. Let us evaluate the merit offered by the number of legs from the viewpoint of specific resistance. When both four-legged and six-legged walking machines are assumed to be similar in size and leg form, and walking at the same speed, Fig. 12 indicates that four-legged walking machines essentially consume greater energy. Of course, the difference shown in Fig. 12 is based on an assumption that the mass ratio $\hat{m}$ is equal. The alternate long and short dotted line of Fig. 12 shows the calculation

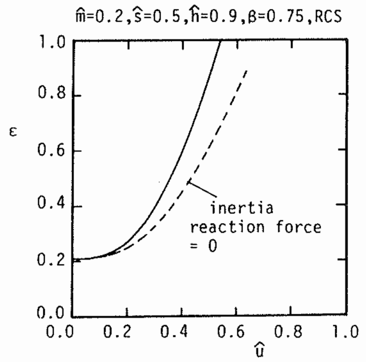

Fig. 10. Specific resistance. The dotted line indicates the data in which the inertia reaction force by the ground is neglected, while it is considered in the solid line.

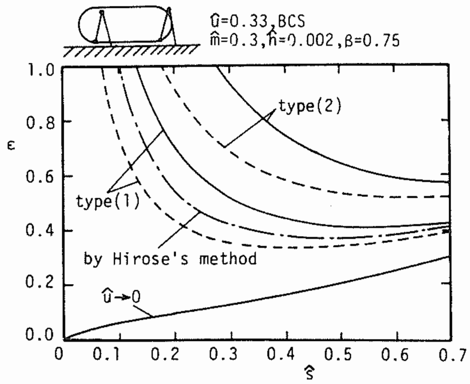

Fig. 11. Specific resistance. The inertia reaction force by the ground is considered in the solid line, while it is not considered in the dotted line and the alternate long and short dotted line.

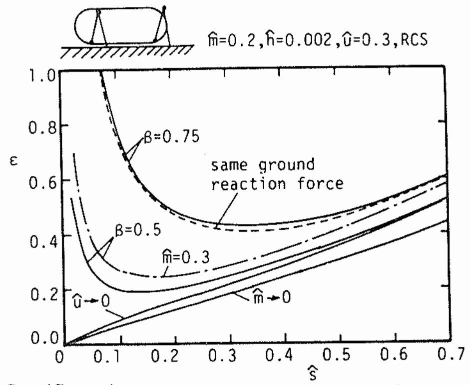

Fig. 12. Specific resistance (parameter: duty factor β). The same ground reaction force is assumed in the dotted line. $\hat{m} = 0.3$ is selected in the alternate long and short dotted line.

results that assumption that $\hat{m}$ of a four-legged walking machine was 0.2 and that $\hat{m}$ of a six-legged walking machine was 0.3 in proportion to the number of legs, prepared for general comparison purposes. Although the difference between $\beta = 0.75$ (the minimum value of a four-legged walking machine) and $\beta = 0.5$ (the minimum value of a six-legged walking machine) becomes small, the qualitative characteristics do not change. However, when $\hat{u} \to 0$, a six-legged walking machine consumes greater energy than a four-legged machine due to the energy consumption resulting from the potential energy change of the leg system. The dotted line represents the calculation results based on an assumption that the ground reaction force acts evenly on all the legs in the support phase. From those facts, it is clear that the ground reaction force distribution effect is not so significant.

Fig. 13 shows the results of examination of the mass ratio $\hat{m}$ effect using the time chart for type 1. Fig. 13 indicates that, for the same stride, a relationship represented by $\epsilon - \epsilon_0 = k\hat{m}$ exists, where ϵ_0 is the specific resistance for $\hat{m} = 0$. This fact corresponds to the phenomenon that the leg mass is a linear function of the joint moment.

Fig. 13 shows not only the calculation results for $n = 4$ (solid line) but also that of $n = 6$ (dotted line) to check that the number of legs n affects the results only slightly. In this case, the maximum difference between $n = 4$ and $n = 6$ is three percent and 1.5 percent on the average. Although cases for $n \geqq 8$ should be examined, because the results will not be changed remarkably even if the number of legs is unnecessarily increased, $n = 6$ is considered satisfactory.

Fig. 14 shows the results of examination of nondimensional velocity $\hat{u}$ effects for a mammal type walking model having RCS actuator arrangement, using the time chart for type 1. The reason why the asymptote for $\hat{u} \to 0$ becomes $\epsilon \fallingdotseq 0$ with $\hat{s} \to 0$ is the same for the fact that, in Fig. 9(c), $\epsilon = 0$ is not available with $\hat{s} \to 0$. (Refer to Appendix D).

As all the calculation results are indicated in nondimensional parameters (Figs. 9–14), results can be applied to every scale of walking machine.

Now let us consider the sensitivity of the results for assumptions. The number of legs in the support phase and the distribution of support forces are not so important factors for the sensitivity of the results as shown in Figs. 12 and 13. Accordingly, the influences caused by assumptions 4-7 are negligible small. The consumed energy due to the up-and-down motions of the center of gravity of each leg is also negligibly small for the usual nondimensional mass ratio, which can be recognized from no remarkable difference between $\hat{u} \to 0$ and $\hat{m} \to 0$ in Fig. 12. Therefore the assumption 3 is also negligible.

On the other hand, since a mass of body is much larger than that of all legs, the consumed energy will remarkably increase with the body acceleration, deceleration, and up-and-down motion. However, these situations are only limited to the starting period, stopping period, and avoiding obstacles in irregular terrain. In normal walking, a body is so controlled that it may keep its velocity and absolute height constant. Therefore, assumption 2 will ensure validity in normal walking.

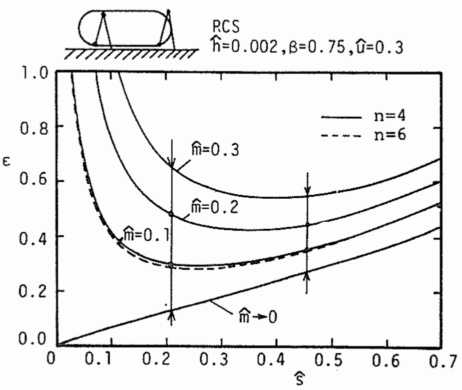

Fig. 13. Specific resistance (parameter: mass ratio $\hat{m}$). Four-legged model is selected in the solid line, while six-legged model is selected in the dotted line.

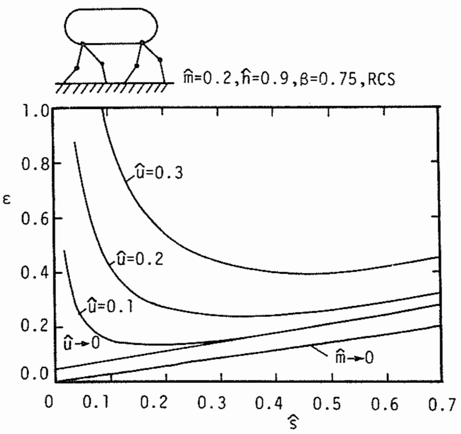

Fig. 14. Specific resistance (parameter: nondimensional velocity $\hat{u}$).

G. An Example of Functional Form $\epsilon = \epsilon(\hat{m}, \hat{s}, \hat{h}, \hat{u}, \beta)$

In this section the functional form of ϵ is considered using the results of the simulation tests discussed in the preceding section. As it is very difficult to express ϵ in universal form, the discussion in this section is limited to a case of an insect type with RCS actuator arrangement ($\hat{h} \to 0$). As the above condition fixes the nondimensional number $\hat{h}$, ϵ is regarded as the function constituents of $\hat{m}$, $\hat{s}$, $\hat{u}$, and β.

Now, then, the specific resistance ϵ of walking machines of this study is considered to consist of the following three terms:

Term 1: A term based on the kinetic energy of the leg system $\to \epsilon_1$

Term 2: A term based on the potential energy generated by the vertical motion of the center of gravity of the leg system $\to \epsilon_2$

Term 3: A term corresponding to the positive work of the actuator against the ground reaction force $\to \epsilon_3$.

Kinetic energy E_l of the leg system consumed by actuators can be expressed by the maximum kinetic energy of the leg system seen from the body as $E_l \sim m_2\{\beta/(1 - \beta)\}^2\bar{u}^2$, and expressed in a form of the specific resistance using k_1 for a constant as $\epsilon_1 = k_1\beta\hat{m}\{\beta/(1 - \beta)\}^2\hat{u}^2/\hat{s}$. On the other hand, it is known from Fig. 12 that ϵ_2 and ϵ_3, based on terms 1 and 2, are expressed as $\epsilon_2 = k_2q(\hat{m})$ and $\epsilon_3 = k_3\hat{s}$, respectively. Furthermore, k_3 is 0.5 according to linear analysis. Now, as the energy consumption due to vertical motion of the center of gravity of the leg system is in proportion to $\hat{m}$, $q(\hat{m})$ is expressed by $q(\hat{m}) \sim \hat{m}$. If it is assumed that the overall specific resistance is expressed as the sum of ϵ_1, ϵ_2, and ϵ_3, the

$$\epsilon = f_1(\hat{m}, \beta)\frac{\hat{u}^2}{\hat{s}} + f_2(\hat{m})\hat{s} \tag{24}$$

where

$$f_1(\hat{m}, \beta) = k_1\hat{m}\frac{\beta^3}{(1-\beta)^2} \tag{25}$$

$$f_2(\hat{m}) = k_2\hat{m} + k_3. \tag{26}$$

As (24) has k_1 and k_2 as unknown quantity, a solution can easily be obtained using two appropriate sets of numerical values for $\hat{m}$, $\hat{s}$, and $\hat{u}$. Thus $k_1 = 0.56$ and $k_2 = 1.01$ are obtained. Figs. 15–17 show the results of verification of each parameter to the extent approximate calculation results are available. It is clear that although (24) is obtained using rough approximation, fairly accurate approximation of the calculation results is available by selecting appropriate k_1 and k_2 values. In addition, since (24) is very simple as compared with the equations used for simulation tests, theoretical specific resistance ϵ can easily be calculated by preparing a fixed equation such as (24) for a typical leg.

After all, there are two primary energy related factors considered here. First is the occurrence of vertical foot force ($k_3\hat{s}$). This results in large bidirectional transfers of energy through the joint actuators even if the vehicle center of gravity is not moving vertically and there is no horizontal foot force required to propel the machine. Second is the bidirectional transfer of energy through the actuators due to acceleration of leg inertias

$$\left(k_1\hat{m}\frac{\beta^3}{(1-\beta)^2}\cdot\frac{\hat{u}^2}{\hat{s}}\right)$$

and vertical motion ($k_2\hat{m}\hat{s}$) of the leg centers of gravity during the stride cycle. Some of the most advanced walking machines [1], [4], [11], [12] in existence totally eliminate the first factor ($k_3 \to 0$) by incorporating gravitationally decoupled actuating system [12].

IV. An Interpretation of Similarity Law

Let us assume two models, model 1 and 2, which are different in size but in perfect geometrical similarity. If as far as the gait pattern is the same, relations $\hat{h}_1 = \hat{h}_2$, $\hat{s}_1 = \hat{s}_2$, and $\beta_1 = \beta_2$ are valid. Now assuming that $\hat{m}_1 = \hat{m}_2$ and the sizes differ by k times ($l_1/l_2 = k$), it is only when $\bar{u}_1 = \sqrt{k}\,\bar{u}_2$ that the specific resistance of model 1 and 2 become theoretically the same. That is to say, the specific resistances of two similar walking machines differ when the sizes of the machines are not the same, and the specific resistances become the same only under limited operating conditions.

V. Conclusion

This paper uses specific resistance as the evaluation index of energetic efficiency, conducted investigations of the similarity law of walking machines, including simulation tests, from a viewpoint of specific resistance. This work has determined the following results.

1) Specific resistance ϵ can be expressed by a function of five nondimensional parameters, mass ratio $\hat{m}$, nondimensional height $\hat{h}$, stride ratio $\hat{s}$, duty factor β, and nondimensional velocity $\hat{u}$.
2) The effect of nondimensional height $\hat{h}$ on the specific resistance is quite remarkable. In the case of a mammal type walking machine, the greater $\hat{h}$, the smaller the specific resistance for the same stride. And in the case of an insect type walking machine, the phenomenon is reversed; i.e., the smaller $\hat{h}$, the smaller the specific resistance.

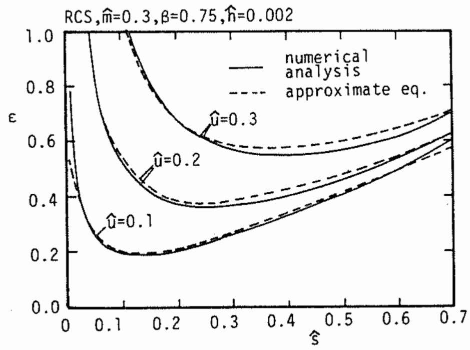

Fig. 15. Comparison between numerical analysis and approximate equation ($\hat{m}$, β, $\hat{h}$ are fixed).

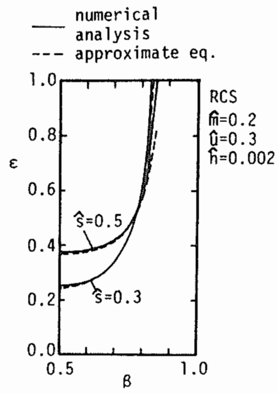

Fig. 16. Comparison between numerical analysis and approximate equation ($\hat{m}$, $\hat{u}$, $\hat{h}$ are fixed).

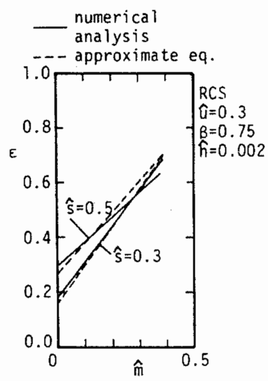

Fig. 17. Comparison between numerical analysis and approximate equation ($\hat{u}$, β, $\hat{h}$ are fixed).

3) For same stride ratio, the effect of the mass ratio $\hat{m}$ on the specific resistance is linear.
4) The consumed energy of the actuator due to the ground inertia reaction force generated by the acceleration motion of the leg system cannot be neglected when the walking speed increases.
5) When four-legged and six-legged walking machines using the same legs are operated at the same speed, the specific resistance of the six-legged walking machine generally decreases at high speed because the duty factor can be reduced to 0.5. At low speed, the specific resistance of the four-legged machine decreases.
6) When two walking machines, 1 and 2, have the same leg mass ratio $\hat{m}$ and are geometrically similar, the specific resistances of both machines become the same when $u_1 = \sqrt{k}\bar{u}_2$, where $\bar{u}$ is the average walking speed and k is the similarity ratio (l_1/l_2).

Appendix A

RCS Type Arrangement

$$A_i=\begin{bmatrix} \frac{4}{3}ml^2+\frac{1}{2}ml^2\cos(\theta_{i1}-\theta_{i2}) & \frac{1}{3}ml^2+\frac{1}{2}ml^2\cos(\theta_{i1}-\theta_{i2}) \\ \frac{1}{2}ml^2\cos(\theta_{i1}-\theta_{i2}) & \frac{1}{3}ml^2 \end{bmatrix} \tag{A1}$$

$$B_i=\begin{bmatrix} ml^2\sin(\theta_{i1}-\theta_{i2}) & \frac{1}{2}ml^2\sin(\theta_{i1}-\theta_{i2}) \\ -\frac{1}{2}ml^2\sin(\theta_{i1}-\theta_{i2}) & 0 \end{bmatrix} \tag{A2}$$

$$C_i=\begin{bmatrix} \frac{2}{3}mgl & \frac{1}{2}mgl \\ 0 & \frac{1}{2}mgl. \end{bmatrix} \tag{A3}$$

$$D_i=\begin{bmatrix} -l(\cos\theta_{i1}+\cos\theta_{i2}) & -l(\sin\theta_{i1}+\sin\theta_{i2}) \\ -l\cos\theta_{i2} & -l\sin\theta_{i2} \end{bmatrix} \tag{A4}$$

BCS Type Arrangement

$$A_i=\begin{bmatrix} \frac{4}{3}ml^2 & \frac{1}{2}ml^2\cos(\theta_{i1}-\theta_{i2}) \\ \frac{1}{2}ml^2\cos(\theta_{i1}-\theta_{i2}) & \frac{1}{3}ml^2 \end{bmatrix} \tag{A5}$$

$$B_i=\begin{bmatrix} -\frac{1}{2}ml^2\sin(\theta_{i1}-\theta_{i2}) & \frac{1}{2}ml^2\sin(\theta_{i1}-\theta_{i2}) \\ -\frac{1}{2}ml^2\sin(\theta_{i1}-\theta_{i2}) & 0 \end{bmatrix} \tag{A6}$$

$$C_i=\begin{bmatrix} \frac{3}{2}mgl & 0 \\ 0 & \frac{1}{2}mgl \end{bmatrix} \tag{A7}$$

$$D_i=\begin{bmatrix} -l\cos\theta_{i1} & -l\sin\theta_{i1} \\ -l\cos\theta_{i2} & -l\sin\theta_{i2} \end{bmatrix}. \tag{A8}$$

Appendix B

The RCS type arrangement is expressed by (A9), which explains the relationship between α_{ij} and θ_{ij} according to Fig. 4. Thus

$$\begin{cases} \alpha_{i1}=\theta_{i1}+\frac{\pi}{2} \\ \alpha_{i2}=\theta_{i2}-\theta_{i1}+\pi. \end{cases} \tag{A9}$$

Therefore, K is given by (A10) when expressed by the relation of $\dot{\alpha}_i$ and $\dot{\theta}_i$:

$$K=\begin{bmatrix} 1 & 0 \\ -1 & 1 \end{bmatrix} \tag{A10}$$

Similarly, K' for the BCS type arrangement is given by

$$K'=\begin{bmatrix} 1 & 0 \\ 0 & 1 \end{bmatrix} \tag{A11}$$

Appendix C

When the leg mass is zero, the sum of the work of the hip joint and the knee joint is always zero. As the body moves in a direction perpendicular to the direction of the machine support force, the machine-support force performs no work against the system. Taking the above facts into consideration and referring to [7] and model of actuators (5), the specific resistance of RCS type leg arrangement is determined by

$$\epsilon=\frac{1}{\hat{s}}\int_{\hat{x}_1}^{\hat{x}_1}|R(\hat{x},\hat{h})|\,d\hat{x} \tag{A12}$$

$$R(\hat{x},\hat{h})=\frac{\hat{h}\hat{x}}{\hat{x}^2+\hat{h}^2}+\frac{\hat{x}^2}{(1-\hat{x}^2-\hat{h}^2)^{1/2}(\hat{x}^2+\hat{h}^2)^{1/2}} \tag{A13}$$

where coordinate x has its origin at the hip and is positive in the forward direction ($\hat{x} = x/2l$).

On the other hand, in the case of the BCS type, the integrand is expressed by

$$B(\hat{x},\hat{h})=\frac{1}{2}\left\{-\frac{\hat{h}^2(1-\hat{x}^2-\hat{h}^2)^{1/2}}{(\hat{x}^2+\hat{h}^2)^{3/2}}+\frac{\hat{x}^2}{(1-\hat{x}^2-\hat{h}^2)^{1/2}(\hat{x}^2+\hat{h}^2)^{1/2}}\right\}. \tag{A14}$$

Then, assuming that the stride is sufficiently small as compared with the length of the leg ($s/2l \ll 1$), an approximate solution is obtained by neglecting terms beyond $\hat{x}^2$:

$$\hat{h} \to 0 \text{ RCS}, \qquad \epsilon \doteqdot \frac{1}{2}\hat{s} \tag{A15}$$

$$\hat{h} \to 0 \text{ BCS}, \qquad \epsilon \doteqdot \frac{1}{4}\hat{s} \tag{A16}$$

$$\hat{h} > 0.5 \text{ RCS}, \qquad \epsilon \doteqdot \frac{1}{4}\frac{\hat{s}}{\hat{h}} \tag{A17}$$

Appendix D

Consumed energy E, when simplified, can be expressed by the product of joint moment M and joint angular change $\Delta\alpha$ as shown by (A18). Hip joint and knee joint are considered for joint angular change, but when $\hat{m} = 0$, as the external work of both joints is always the same with opposite signs, taking up only the hip joint will not lose universality:

$$E \sim M \cdot \Delta\alpha. \tag{A18}$$

In the case of the RCS type and insect type leg arrangements, joint moment M and angular change $\Delta\alpha$ are considered $M \propto s$, $\Delta\alpha \propto s$. Therefore the specific resistance for $\hat{s} = 0$ is represented by (A19).

$$\epsilon = \lim_{s \to 0} \frac{ks^2}{m_1 gs} = 0. \tag{A19}$$

In the case of mammal type BCS arrangement, as the hip joint moment does not become zero even if $s = 0$ (refer to Section III-A), $M = k_1 + k_2 s$ and $\Delta\alpha \propto s$ are obtained. Therefore the specific resistance for $s = 0$ is expressed by

$$\epsilon = \lim_{s \to 0} \frac{k_1 s(k_1 + k_2 s)}{m_1 gs} \not\doteqdot 0. \tag{A20}$$

The above-mentioned philosophy is the physical basis for $\epsilon \doteqdot 0$ if $s = 0$. A similar philosophy applies to mammal type RCS ($m \doteqdot 0$). In this case, $\epsilon \doteqdot 0$ if $s = 0$ because the leg mass normally generates moment about the hip joint.

Acknowledgment

Finally, the authors would like to extend their sincere thanks to Professor R. B. McGhee of the Ohio State University for his valuable assistance, including the methods for approaching indeterministic problems.

Nomenclature

B	movement of center of gravity of body during one cycle
E	energy consumption by actuators during one cycle
g	gravitational acceleration
h, $\hat{h}$	body height, nondimensional body height
H_i	horizontal ground reaction force in ith leg
k	similarity ratio
l	leg unit length
m_1, m_2, $\hat{m}$	mass of body, mass of one leg, nondimensional mass ratio
M_{i_1}, M_{i_2}	hip joint moment of ith leg, knee joint moment of ith leg
n, n_1, n_2	number of legs, number of legs in support phase at even-number leg row, number of legs in support phase at odd-number leg row
P	power consumption in joint actuator
s, $\hat{s}$	stride length, stride ratio
T_0	walking period
$\bar{u}$, $\hat{u}$	average walking velocity, nondimensional velocity
V_i	vertical ground reaction force in ith leg
X_i, X_{bi}	x-directional component of ith leg inertia force, x-directional component of ith body reaction force
Y_i, Y_{bi}	y-directional component of ith leg inertia force, y-directional component of ith leg body reaction force
ϵ	specific resistance
β	duty factor.

References

[1] K. J. Waldron, *et al.*, "Configuration design of the adaptive suspension vehicle," *Int. J. Robotics Res.*, vol. 3, no. 2, pp. 37–48, 1984.
[2] G. Gabrielle and T. Karman, "What price speed?" *Mechanical Engineering*, vol. 72, no. 10, p. 775, 1950.
[3] M. G. Bekker, *Introduction to Terrain-Vehicle Systems.* Ann Arbor, MI: Univ. of Michigan, p. 417, 1969.
[4] M. Kaneko, M. Abe, and K. Tanie, "A hexapod walking machine with decoupled freedoms," *IEEE J. Robotics Automat.*, vol. 1, no. 4, pp. 183–190, 1985.
[5] T. Frank, "Dynamic study of a four-bar linkage walking machine leg," M.S. thesis, Ohio State University, p. 133, 1973.
[6] S. Hirose and Y. Umetani, "The basic considerations on energetic efficiencies of walking vehicles," *Trans. Soc. Instrument Contr. Engineers* (in Japanese), vol. 15, no. 7, pp. 928–933, 1979.
[7] T. J. Pedley, *Scale Effect in Animal Locomotion.* New York: Academic, p. 93, 1977.
[8] A. A. Gukhman, *Introduction to the Theory of Similarity.* New York: Academic, 1965.
[9] C. A. Klein *et al.*, "Use of force and attitude sensors for locomotion of a legged vehicle over irregular terrain," *Int. J. Robotics Res.*, vol. 2, no. 3, pp. 2–17, 1983.
[10] A. Gelb, *Applied Optimal Estimation.* Cambridge, MA: MIT, p. 19, 1979.
[11] T. G. Bartholet, "The first functionoid developed by ODETICS. INC.," in *Proc. ICAR Symp.*, pp. 293–298, 1983.
[12] S. Hirose, "A study of design and control of a quadruped walking vehicle," *Int. J. Robotics Res.*, vol. 3, no. 2, pp. 37–48, 1984.

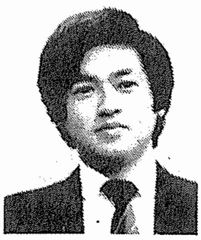

Makoto Kaneko (A'84) was born on January 18, 1954 in Hagi, Yamaguchi Prefecture, Japan. He received the B.S. degree from the Kyushu Institute of Technology in 1976 and the M.S. and D.S. degrees in mechanical engineering from the University of Tokyo in 1978 and 1981, respectively.

Since 1981 he has been a researcher of the Mechanical Engineering Laboratory, Ministry of International Trade and Industry at Tsukuba Science City and is currently a Senior Research Scientist of Cybernetics Division of the Department of Robotics. His current interests include robotics.

Dr. Kaneko is a member of the Japan Society of Mechanical Engineers, the Society of Instrument and Control Engineers, the Society of Biomechanisms, and the Robotics Society of Japan. He received a Young Engineer Award for the study on self-excited oscillation of two phase pumping system from the Japanese Society of Mechanical Engineers in 1984.

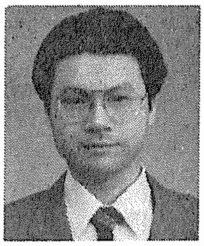

Susumu Tachi (M'82) was born in Tokyo, Japan, on January 1, 1946. He received the B.E., M.S., and Ph.D. degrees in mathematical engineering and instrumentation physics from the University of Tokyo, Tokyo, Japan, in 1968, 1970, and 1973, respectively.

He joined the Faculty of Engineering, University of Tokyo, in 1973. From 1973 to 1976 he held a Sakkokai Foundation Fellowship. In 1975 he joined the Mechanical Engineering Laboratory, Ministry of International Trade and Industry, Tsukuba Science City, Japan, and he is currently Director of the Man-Machine Systems Division, Robotics Department. Since 1983 he has been Associate Director of the National Robotics Project. From 1979 to 1980 he was a Japanese Government Award Senior Visiting Fellow at the Massachusetts Institute of Technology, Cambridge. His present interests in robotics include navigation of autonomous mobile robots, sensory control of robots, rehabilitative robotics (MELDOG), and human robot systems (Tele-existence).

Dr. Tachi is a founding director of the Robotics Society of Japan. He is a member of the Japan Society of Medical Electronics and Biomedical Engineering, the Society of Instrument and Control Engineers, the Japan Society of Mechanical Engineers, and the Society of Biomechanisms.

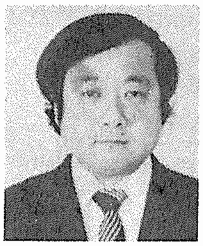

Kazuo Tanie (M'85) was born in Yokohama, Japan, on November 6, 1946. He received the B.S., M.S., and Dr.Eng. degrees in mechanical engineering from Waseda University, Tokyo, Japan, in 1969, 1971, and 1980, respectively.

He joined the Mechanical Engineering Laboratory, Ministry of International Trade and Industry, Tsukuba Science City, Japan, in 1971, and he is currently the Director of Cybernetics Division of the Department of Robotics. He was a Visiting Scholar of the Biotechnology Laboratory, the University of California at Los Angeles, from August 1981 to August 1982. His interests currently relate to tactile sensor, mechanisms, and control in robotics.

Dr. Tanie is a member of the Board of Directors of the Robotics Society of Japan. He is a member of Advisory Board of the Society of Biomechanisms, and the Japan Ergonomics Research Society. He is a member of the Japan Society of Mechanical Engineers, the Society of Instrument and Control Engineers, and the Japan Association of Automatic Control Engineering.

Minoru Abe was born in Tokyo, Japan, on August 11, 1932. He received the B.S. degree in mechanical engineering in 1955 from Yokohama National University, Yokohama, Japan.

He joined the Mechanical Engineering Laboratory, Ministry of International Trade and Industry, Tsukuba Science City, Japan, in 1955. He has been engaged in research and development on mechanisms of machine elements and robotics. His major research interests are in rehabilitation engineering. He is currently the director of the Department of Robotics, the Mechanical Engineering Laboratory, Japan.

Mr. Abe is a member of the Japan Society of Mechanical Engineers, the Society of Instrument and Control Engineers, the Society of Biomechanisms, the Japan Society of Medical Electronics and Biomedical Engineering, and the Robotics Society of Japan.